Dynamics of viscous penetration in percolation porous media

J. S. Andrade, Jr.,[1,2] A. D. Araújo,[2] S. V. Buldyrev,[1] S. Havlin,[1,3] and H. E. Stanley[1]
[1]*Center for Polymer Studies, Boston University, Boston, Massachusetts 02215*
[2]*Departamento de Física, Universidade Federal do Ceará, 60451-970 Fortaleza, Ceará, Brazil*
[3]*Minerva Center & Department of Physics, Bar-Ilan University, Ramat Gan, Israel*
(Received 25 September 2000; published 25 April 2001)

We investigate the dynamics of viscous penetration in two-dimensional percolation networks at criticality for the case in which the ratio between the viscosities of displaced and injected fluids is very large. We report extensive numerical simulations that indicate that the scaling exponents for the breakthrough time distribution are the same as the previously reported values computed for the case of unit viscosity ratio. Our results are consistent with the possibility that viscous displacement through critical percolation networks constitutes a single universality class, independent of the viscosity ratio. We also find that the distributions of mass and breakthrough time of the invaded clusters have the same scaling form, but with different critical exponents.

DOI: 10.1103/PhysRevE.63.051403 PACS number(s): 47.55.Mh, 05.45.Df, 61.43.Hv, 64.60.Ak

I. INTRODUCTION

The interesting physics related to the displacement phenomenon of a viscous fluid by a less viscous one inside a porous material has been the subject of intensive research in the past and in recent years, in particular due to its close connections with hydrology and oil recovery [1,2]. These studies have been fairly successful in describing the complex geometrical features of the displacement structures in terms of statistical mechanical models, such as invasion percolation (IP), viscous fingering (VF), and diffusion-limited aggregation (DLA) [3–6]. More recent works on this subject have been motivated by the rich variety of intriguing phenomena that the invasion process can display, such as avalanches and flux front roughening [7,8]. All these studies unambiguously indicate that the morphological characteristics of objects generated during the displacement process (e.g., the invading cluster or the penetration front) should be strongly dependent on the physicochemical and operational properties of the flow.

Just at the critical point, the incipient infinite percolation cluster [9,10] is an example of a random fractal that has been extensively used as a convenient paradigm for real disordered systems. An obvious advantage of using the percolation model is that a comprehensive set of exactly and numerically calculated critical exponents is now available to describe most of its geometrical and transport features. In addition, it is well established that the electrical transport in disordered media with a *broad* distribution of conductance values is dominated by those regions where the conductances are larger than some critical value [11]. This value is the largest conductance such that the set of conductances above this threshold still preserves the global connectivity of the system. In percolation terminology, this is equivalent to working with the conducting spanning cluster. Known as ''the critical path method,'' this powerful approximation has been successfully applied [12] to estimate transport properties (e.g., permeability and electrical conductivity) of disordered porous materials.

Only a few studies have been devoted to the investigation of the displacement process through percolation porous media *at criticality*. Murat and Aharony [13] showed by numerical simulation with two-dimensional diluted percolation lattices that, although the clusters generated from VF and DLA have the same fractal dimension at the vicinity of the critical point, many other geometrical differences can be observed between these two processes. In two recent studies [14,15], the dynamics of viscous displacement through percolation porous media has been investigated in the limiting condition of unitary viscosity ratio, $m \equiv \mu_2/\mu_1 = 1$, where μ_1 and μ_2 are the viscosities of the injected and displaced fluids, respectively. In this situation, the displacement front can be approximately modeled by tracer particles that follow the streamlines of the flow. As a result, it was shown that the distributions of the shortest path and minimal traveling time of the tracer closely obey a proposed scaling *ansatz* [16,17] that can account for both the effect on L—the finite size of the system—and on p, the bond occupancy probability.

The main purpose of the present study is to investigate the detailed dynamics of viscous penetration through two-dimensional (2D) critical percolation networks in the limiting case of a very large viscosity ratio, $m \to \infty$. The organization of the paper is as follows. In Sec. II, we present the characteristics of the theoretical model and related parameters. The results are shown and discussed in Sec. III and the concluding remarks are then presented in Sec. IV.

II. MODEL FORMULATION

The porous media is modeled here by bond percolation on a square lattice with sites that have negligible volume and bonds that are cylindrical tubes of fixed length ℓ_p and radius r_p. We consider the percolation backbone generated at the critical point between two sites (''wells'') W_1 and W_2 separated by a fixed distance r (see Fig. 1). As a macroscopic boundary condition, a constant pressure drop $\Delta p = p_{W1} - p_{W2}$ is imposed between the injecting (W_1) and extracting wells (W_2) during the dynamics. For simplicity, we consider here the case in which capillary forces are locally negligible in the system. This is analogous to assuming that the interfacial pressure drop between fluids is negligible at each pore [3]. In addition, the tubes connecting the sites are sufficiently

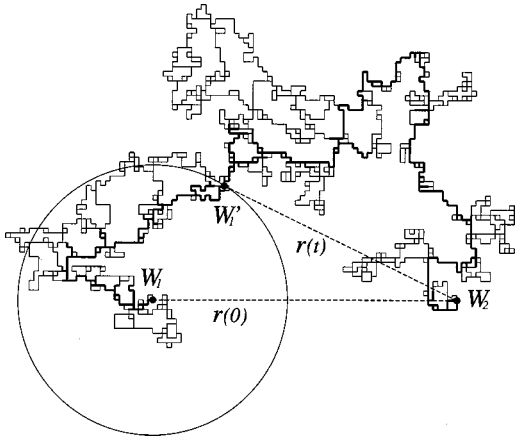

FIG. 1. Pictorial representation of the viscous penetration process in a typical percolation network of pores. A constant pressure drop Δp is applied between the points W_1 and W_2 separated by the distance r. At initial time, the entire network is filled with a fluid of finite viscosity (displaced fluid). The invading fluid of zero viscosity penetrates through W_1 and reaches W_2 at the breakthrough time t_b. The thin lines correspond to pores filled with the displaced fluid, while the thick lines are the pores filled with the invading fluid at $t=t_b$.

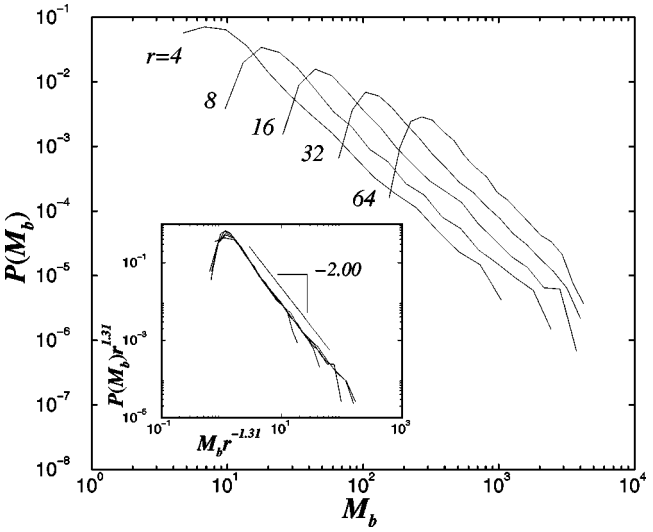

FIG. 2. Logarithmic plot of the distribution of mass of invaded clusters $P(M_b)$ for different distances $r=4,8,16,32,64$ between injection (W_1) and extraction (W_2) points. The inset shows the collapsed data obtained by rescaling the mass M_b with its corresponding characteristic value $M_b^* \sim r^{1.31}$. The least-square fit to the data in the scaling region gives $g_M = 2.00 \pm 0.04$.

long, $\ell_p \gg r_p$, to assume that the flow between nodes i and j at the pore scale follows Hagen-Poiseuille's law,

$$q_{ij} = \frac{\pi r_p^4}{8\mu(\ell_p - x_{ij})}(p_i - p_j) = g_{ij}(p_i - p_j). \tag{1}$$

Here p_i is the pressure at node i, q_{ij} is the volumetric flow rate between nodes i and j, g_{ij} is the hydraulic conductance of the pore, and μ is the viscosity of the displaced fluid. The local variable x_{ij}, $0 \leqslant x_{ij} \leqslant \ell_p$, is a time-dependent length that corresponds to the part of the pore that is filled with the displacing fluid during the penetration process. Mass conservation at each node of the lattice leads to the following set of linear algebraic equations:

$$\sum_j q_{ij} = \sum_j g_{ij}(p_i - p_j) = 0 \quad \text{for} \quad i = 1,2,\ldots,N, \tag{2}$$

where N is the number of sites. Note that because $g_{ij}^{-1} = 0$, the pressure inside the invaded region must be everywhere equal to the pressure p_{W1} applied at the well W_1. In order to simulate the dynamics of viscous invasion, we compute the local displacement in each pore at the front as $\Delta x_{ij} = q_{ij}\Delta t_{\min}/\pi r_p^2$, where $\Delta t_{\min}$ is the variable time step of the process, calculated as the minimum value among all the interface pores, necessary for the invading fluid to reach a new node. Accordingly, we keep updating the front and recalculating the pressure field until the displacing fluid reaches the second well W_2. At this point, we record the mass M_b of the invaded cluster and the breakthrough time t_b, i.e., the total time for the invading front to move from W_1 to W_2. For a fixed value of r, this operation is repeated for 10 000 network realizations of size $L \times L$, where $L = 500 \gg r$. We run these simulations for different values of r and find that there is always a well-defined region where the distributions of M_b and t_b follow the scaling form [16]

$$P(z) = A_z \left(\frac{z}{z^*}\right)^{-g_z} f\left(\frac{z}{z^*}\right), \tag{3}$$

where z denotes M_b or t_b, z^* is the maximum of the probability distribution, the normalization constant is given by $A_z \sim (z^*)^{-1}$, and the scaling function has the form [14,15]

$$f(y) = \exp(-a_z y^{-\phi_z}). \tag{4}$$

The exponents ϕ_z and d_z are related by

$$\phi_z = \frac{1}{d_z - 1}. \tag{5}$$

Note that the scaling function f decreases sharply when z is smaller than z^*. The lower cutoff is due to the fact that the mass M_b cannot be smaller than the mass of invading fluid filling a single straight tube of radius r_p and length r.

III. RESULTS AND DISCUSSION

In Figs. 2 and 3, we show the log-log plots of the distributions $P(M_b)$ and $P(t_b)$, respectively, for five different values of the well distance: $r=4$, 8, 16, 32, and 64. For each curve, we determine the characteristic size z^* as the peak of the distribution and plot z^* versus the distance r in double-logarithmic scale. As shown in Fig. 4, the results of our simulations indicate that both M_b^* and t_b^* have a power-law dependence on the distance r, $z^* \sim r^{d_z}$. The linear fit to the data yields the exponents d_z for each distribution, namely

$$d_M = 1.31 \pm 0.02 \tag{6}$$

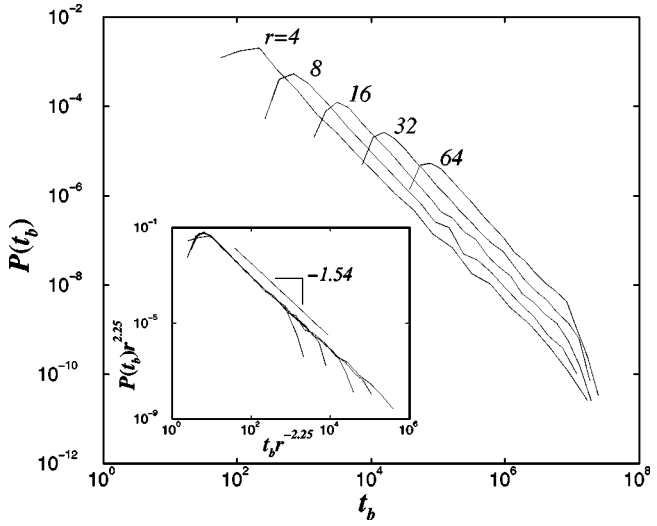

FIG. 3. Logarithmic plot of the breakthrough time distribution $P(t_b)$ for $r=4,8,16,32,64$. The inset shows the collapsed data obtained by rescaling the time t_b with its corresponding characteristic value $t_b^* \sim r^{2.25}$. The least-square fit to the data in the scaling region gives $g_t = 1.54 \pm 0.03$.

and

$$d_t = 2.25 \pm 0.03. \tag{7}$$

In particular, the exponent d_M is the fractal dimension of the invaded cluster. It has been previously estimated by Murat and Aharony [13] using smaller system sizes, a *stochastic* type of invasion algorithm, and a different set of boundary conditions to represent the source and sink of mass. The obtained value $d_M = 1.30 \pm 0.05$, however, is in very good agreement with our result. Paredes and Octavio [18] also obtained a quite similar result for the structure of the injected fluid ($d_M \approx 1.37$) using the invasion percolation model with trapping in percolating clusters.

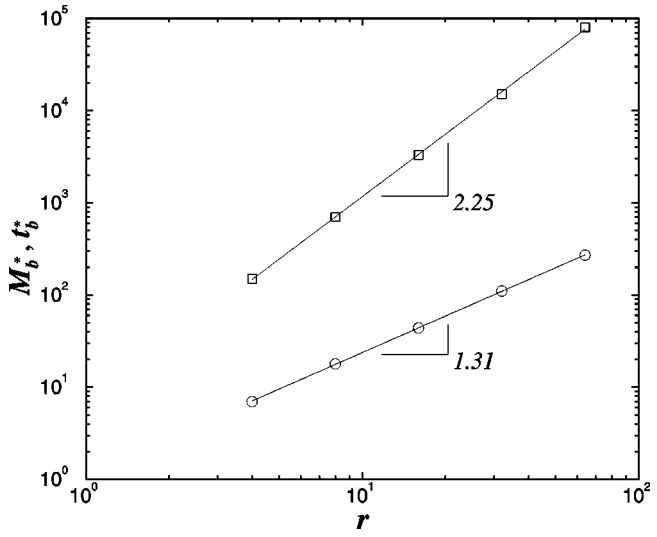

FIG. 4. Log-log plot of the most probable values for the mass of invaded clusters M_b^* (circles) and breakthrough time t_b^* (squares) versus the distance r. The straight lines are the least-square fits to the data, with the numbers indicating the slopes, $d_M = 1.31 \pm 0.02$ (circles) and $d_t = 2.25 \pm 0.03$ (squares).

The insets of Figs. 2 and 3 show the data collapse obtained by rescaling M_b and t_b to their characteristic size, M_b^* and t_b^*, respectively. Both distributions are consistent with the scaling form of Eq. (3). From the least-square fit to the data in the scaling regions, we obtain the exponents $g_M = 2.00 \pm 0.04$ and $g_t = 1.54 \pm 0.03$. At this point, it is important to recall that the breakthrough time exponents reported in [15] for the special case $m=1$ are $d_t \approx 2.3$ and $g_t \approx 1.57$, computed at constant pressure. Furthermore, note that the scaling exponents of the invaded cluster mass g_M and d_M also coincide with the exponents for breakthrough time reported in Ref. [15] for $m=1$ at constant flow. In the case $m=1$, the conductance G of the system is constant over time and scales with the distance r as $G \sim r^{-\zeta}$, with $\zeta \approx 0.975$ [9]. The breakthrough time computed at constant flow t_{bq} coincides with the cluster mass M invaded by the time of the breakthrough. The breakthrough time at constant pressure is given by $t_{bp} = t_{bq}/G$. Accordingly, $t_{bp} \sim r^{d_M+\zeta}$. Hence one expects the relationship $d_t = d_M + \zeta$. Since the values of t_{bp} and t_{bq} are strongly correlated with each other, $t_{bp} \sim t_{bq}^{(d_M+\zeta)/d_M}$, the distributions of both quantities must obey the relationship

$$P(t_{bp})dt_{bp} = P(t_{bq})dt_{bq}, \tag{8}$$

from which it follows that

$$g_t = 1 + (g_M - 1)\frac{d_M}{d_M+\zeta} \approx 1.57. \tag{9}$$

This is in good agreement with the data obtained for $m \to \infty$ as well as for the data obtained in Ref. [15] for $m=1$. The excellent agreement between the exponents obtained for the cases $m \to \infty$ and $m=1$ seems to indicate that the process of viscous penetration in percolation porous media constitutes a single class of universality.

From a practical point of view, it is important to understand the relationship between the dynamical variables M_b and t_b, which in the case $m \to \infty$ is not so simple as in the case $m=1$. Here, we explain this by considering that it is possible to map the statistics over several samples into the dynamics of viscous penetration of a single but sufficiently large pore network realization. In this situation, we can always express the global dynamics of the system in terms of the following mass balance:

$$\frac{dM}{dt} = \rho G \Delta p, \tag{10}$$

where M is the mass of the invaded cluster at time t, ρ is the density of the invading fluid, taken as constant, and G is the overall hydraulic conductance of the pore network. At any time t during the dynamics, the variable G can be calculated as the conductance of the remaining pore space filled with defending fluid. Therefore, G should be of the order of the conductance between the most advanced site in the invading front and the second well W_2. As shown in Fig. 1, this sim-

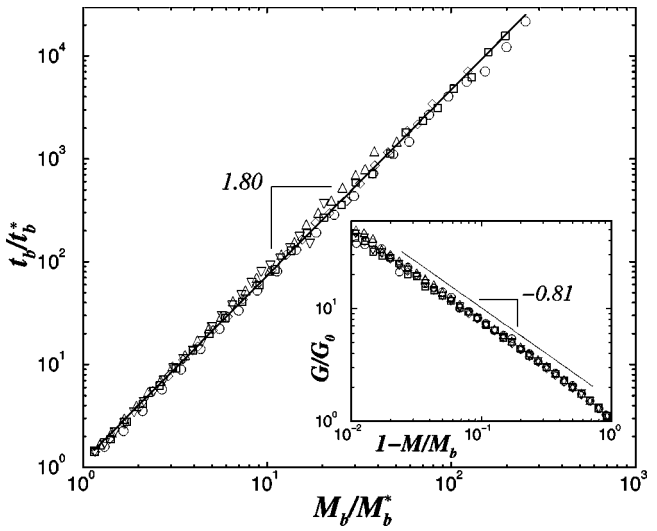

FIG. 5. Power-law dependence of t_b/t_b^* on M_b/M_b^* for $r=4$ (circles), 8 (squares), 16 (diamonds), 32 (up triangles), and 64 (down triangles). Each abscissa is the average over the M_b values falling within the range of a specified logarithmic bin. The ordinate is the average over the corresponding t_b values. The computed error bars are smaller than the symbols. The solid line with slope 1.80 ± 0.04 is the least-square fit to all data sets in the scaling region. The inset shows the power-law behavior of the intrinsic invasion dynamics in terms of $G(t)/G_0$ versus $1-M(t)/M_b$. These data have been obtained by averaging the individual time-dependent process of penetration over 200, 400, 600, 800, and 1000 realizations of 500×500 pore networks generated with $r=4$ (circles), 8 (squares), 16 (diamonds), 32 (triangles up), and 64 (triangles down), respectively.

ply means that the dynamics of the invasion cluster can be approximately followed as a sequence of translations in the first well W_1 to points W_1' located at the front. If we now make use of the scaling relation $G\sim r^{-\zeta}$ and assume that the remaining mass to be filled within the displaced phase is sufficiently large to obey

$$(M_b-M)\sim r^{d_M}, \tag{11}$$

it follows that

$$G\sim(M_b-M)^{-\zeta/d_M}. \tag{12}$$

The substitution of Eq. (12) into Eq. (10) and integration over the entire dynamics gives the following scaling behavior between the breakthrough time and mass:

$$t_b\sim M_b^{\alpha}, \tag{13}$$

where $\alpha=(\zeta+d_M)/d_M\approx1.75$ in two dimensions. In Fig. 5, we show that the logarithmic dependence of t_b on M_b for all values of the distance r used in the simulations can be satisfactorily represented by a single straight line with slope equal to 1.80 ± 0.04. A difference smaller than 3% between predicted and calculated α exponents confirms the validity of our similarity argument. For consistency, it is important to show that the basic assumption (12) used to determine the exponent α is indeed descriptive of the *intrinsic* dynamics of viscous invasion. We therefore carried out additional simulations where the entire penetration dynamics of the percolation pore space is sampled over several lattice realizations. The results displayed in the inset of Fig. 5 show that the average dynamics of the normalized conductance, $G(t)/G_0$, where $G_0=G(0)$, follows a power law,

$$G(t)/G_0\sim\left(1-\frac{M(t)}{M_b}\right)^{-\beta}, \tag{14}$$

with an exponent

$$\beta=0.81\pm0.03. \tag{15}$$

This numerically estimated value is also in good agreement with the theoretical approximation (12), which predicts

$$\beta=\zeta/d_M\approx0.75. \tag{16}$$

IV. CONCLUSION

In summary, we found by numerical simulations on 2D percolation networks at criticality that the scaling *ansatz* proposed in [16,17] to characterize the dynamics of viscous displacement at $m=1$ also holds for the case of very large viscosity ratio, $m\to\infty$. Surprisingly, we found that the distribution exponents g_z and d_z estimated for these two limiting cases are statistically identical. Based on this fact, we suggest that the two processes should belong to the same universality class. Of course, we emphasize that this universal behavior only applies to percolationlike porous media and should not be generalized to the structure of other porous materials. Our results also indicate that the relevant dynamical exponent relating the mass of the displacing cluster and the breakthrough time can be directly obtained from previously known exponents by means of a simple similarity argument. We expect these results to be valid also for real percolation porous media.

ACKNOWLEDGMENTS

We thank N. V. Dokholyan, P. R. King, Y. Lee, G. Paul, G. Sauermann, and A. Scala for fruitful discussions and BP-Amoco, CNPq, NSF, and FUNCAP for financial support.

[1] F. A. L. Dullien, *Porous Media — Fluid Transport and Pore Structure* (Academic Press, New York, 1979).

[2] M. Sahimi, *Flow and Transport in Porous Media and Fractured Rock* (VCH, Boston, 1995).

[3] J.-D. Chen and D. Wilkinson, Phys. Rev. Lett. **55**, 1892 (1985).

[4] A. H. Thompson, A. J. Katz, and R. A. Raschke, Phys. Rev. Lett. **58**, 29 (1987).

[5] A. Coniglio, in *Hydrodynamics of Dispersed Media*, edited by J. P. Hulin, A. M. Cazabat, E. Guyon, and F. Carmona (Elsevier, Amsterdam, 1990), p. 193.
[6] U. Oxaal, F. Boger, J. Feder, T. Jossang, P. Meakin, and A. Aharony, Phys. Rev. A **44**, 6564 (1991).
[7] E. Aker, K. J. Maløy, and A. Hansen, Phys. Rev. E **61**, 2936 (2000); E. Aker, K. J. Maloy, A. Hansen, and S. Basak, Europhys. Lett. **51**, 55 (2000).
[8] C.-H. Lam and V. K. Horvath, Phys. Rev. Lett. **85**, 1238 (2000).
[9] D. Stauffer and A. Aharony, *Introduction to Percolation Theory* (Taylor & Francis, Philadelphia, 1994).
[10] *Fractals and Disordered Systems*, 2nd ed., edited by A. Bunde and S. Havlin (Springer-Verlag, New York, 1996).
[11] V. Ambegaokar, B. I. Halperin, and J. S. Langer, Phys. Rev. B **4**, 2612 (1971).
[12] A. J. Katz and A. H. Thompson, Phys. Rev. B **34**, 8179 (1986); J. Geophys. Res. B **92**, 599 (1987).
[13] M. Murat and A. Aharony, Phys. Rev. Lett. **57**, 1875 (1986).
[14] Y. Lee, J. S. Andrade, Jr., S. V. Buldyrev, N. V. Dokholyan, S. Havlin, P. R. King, G. Paul, and H. E. Stanley, Phys. Rev. E **60**, 3425 (1999).
[15] J. S. Andrade, Jr., S. V. Buldyrev, N. V. Dokholyan, S. Havlin, P. R. King, Y. Lee, G. Paul, and H. E. Stanley, Phys. Rev. E **62**, 8270 (2000).
[16] S. Havlin and D. Ben-Avraham, Adv. Phys. **36**, 695 (1987).
[17] N. V. Dokholyan, Y. Lee, S. V. Buldyrev, S. Havlin, P. R. King, and H. E. Stanley, J. Stat. Phys. **93**, 603 (1998).
[18] R. Paredes and M. Octavio, Phys. Rev. A **46**, 994 (1992).